СООБЩЕНИЯ
ОБЪЕДИНЕННОГО
ИНСТИТУТА
ЯДЕРНЫХ
ИССЛЕДОВАНИЙ
ДУБНА

10/I-77
E1 - 10063

ELASTIC SCATTERING OF $\pi^{\pm}$ p, $K^{\pm}$ p, pp AND $\bar{p}p$ AT 40 GEV/C

1976

E1 - 10063

ELASTIC SCATTERING OF $\pi^{\pm}$ p, $K^{\pm}$ p, pp AND $\bar{p}p$ AT 40 GEV/C

Yu.M.Kazarinov, M.Yu.Kazarinov, B.Khatchaturov, I.Potashnikova, J.Strakhota.

Joint Institute for Nuclear Research.

C.Bruneton, J.Bystricky, G.Cozzika, J.Deregel, Y.Ducros, A.Gaidot, F.Khantine-Langlois, F.Lehar, A.De Lesquen, J.P.Merlo, S.Miyashita, J.Movchet, J.Pierrard, J.C.Raoul, L.VanRossum.

Centre d'Etudes Nucleaires, Saclay, France.

A.Derevschikov, Yu.Matulenko, A.P.Meschanin, S.B.Nurushev, A.Saraykin, V.Siksin, E.Smirnov, V.Solovyanov.

Institute of High Energy Physics, Serpukhov, USSR.

V.P.Kanavets.

Institute of Theoretical and Experimental Physics, Moscow, USSR.

I. INTRODUCTION

The results of the determination of the differential cross sections for elastic $\pi^- p$, $K^- p$, $p^- p$ and $\pi^+ p$, $K^+ p$, pp scattering at 40 and 45 GeV/c, respectively, are presented.

The experiment has been carried out at the Serpukhov accelerator to investigate polarization phenomena in these processes. Polarization and spin rotation parameters have been published previously [1,2]. The statistics used to calculate the differential cross-sections was collected during polarization measurements. The experimental apparatus [3] permitted one to detect elastic scattering events up to $t = -2.5$ (GeV/c)^2, but the t-interval for the differential cross-section of some reactions was decreased by poor statistics.

II. EXPERIMENTAL LAYOUT

The schematic view [3] of the apparatus used in this experiment is shown in Fig. 1.

The scintillation counters T_1, T_2, T_3 measured the number of particles in the beam. The beam direction was determined by the scintillation hodoscope $H_{1,2}$, $H_{3,4}$

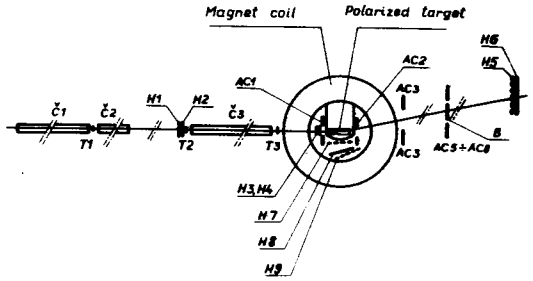

Fig. 1. Experimental layout.

to an accuracy of ±0.38 mrad (HWHM). The negative beam particles were identified by three threshold gas Cherenkov counters. In the case of the positive beam four Cherenkov counters were used.

A polarized target (PT) of propane-diol ($C_3H_8O_2$) was used in this experiment. The measurements with a carbon target were made to subtract the bound proton background.

The hodoscopes H_5 , H_6 measured the direction of the scattered particle to an accuracy of ±0.2 mrad. Over the momentum-transfer region covered, $0.08 \leq |t| \leq 2.5$ $(GeV/c)^2$, the t-resolution changed within the limits of $0.02 \leq |\Delta t| \leq 0.1$ $(GeV/c)^2$, respectively.

The hodoscopes H_7 , H_8 , H_9 were placed in the bore of the target magnet and detected the recoil protons with an azimuthal acceptance of ±16°. Anticoincidence counters AC1-AC8 for charged particles and gamma-rays were placed around the target. Fast electronics selected events with only one pulse from each hodoscope and included coincidence matrices to choose the scattering events with two-body kinematics. The events were recorded on magnetic tape by the CII-90-10 computer.

III. ANALYSIS OF ELASTIC EVENTS

The main steps of the analysis of scattering events recorded on the magnetic tape were as follows:

1. Reconstruction of elastic scattering events.
2. Relative normalization of the number of events obtained with the opposite signs of target polarization.
3. Background subtraction from quasi-elastic scattering on bound protons in nuclei.
4. Background estimation of inelastic scattering on hydrogen.

1. At first the scattering angle of the scattered particle was calculated using information from the hodoscopes H_5 , H_6. Then the trajectories in the magnetic field and the observed angle (Θ_p^m) of the recoil proton were reconstructed using the reading of the H_7 , H_8 , H_9 hodoscopes. The values of the scattering angle and the observed recoil angle Θ_p^m were defined more precisely by the iterative method, taking into account the position of the interaction point. Then the recoil proton angle (Θ_p^c) was calculated from the angle of the scattering particle assuming elastic scattering kinematics of a proton at rest. The histograms representing the angular correlation $N_p^\theta = f(\Delta\Theta_p = \Theta_p^m - \Theta_p^c)$ were built for the given interval of Δt /3/. There are well-pronounced maxima containing the "elastic peaks" (Fig.2).

2. The region outside the "elastic peaks" of the angular distribution was used for the relative normalization of the data with the opposite signs of the target polarization and the carbon data (quasi-elastic scattering background)/3/.

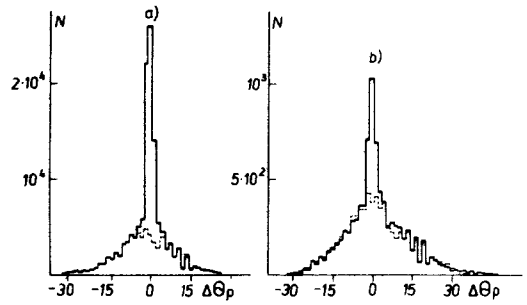

Fig. 2. Selection of elastic scattering events on free protons for two momentum transfer bins: a) $0.32 \leq |t| < 0.38$ $(GeV/c)^2$, b) $1.0 \leq |t| < 1.14$ $(GeV/c)^2$. The solid and dashed histograms show the distribution of $\Delta\Theta_p$ with the polarized target and the dummy target, respectively.

3. The central region of the distribution $N(\Delta\Theta_p)$ was used to define the number of elastic scattering events. The region limits were chosen considering the elastic peak width which is mostly due to the resolution of the detected system. The normalized quasi-elastic scattering background was subtracted from the total number of events inside this region.

4. The background from inelastic scattering on hydrogen was estimated by the Monte Carlo method. The reactions with two charged particles in the final state were the main source of the inelastic background, since the reactions with more than two charged particles and γ were rejected by anticoincidence

counters. In the πp scattering the Monte Carlo calculation for the final states ρp, πN^{*+} and $p\pi\pi^{\circ}\pi^{\circ}$ showed a contribution of smaller than 1% of the total number of elastic events on free protons. The same should take place in the Kp scattering.

In pp scattering the inelastic two-prong events with the additional π in the forward direction give the main contribution to the background. To subtract this background, two different methods were used. In the first case the probability for such events to appear as elastic scattering at various four-momentum transfers is calculated by a Monte-Carlo programme using the data for inelastic pp scattering at high energies [1]. In the second method kinematics selection criteria were strengthened and only the left-hand side of the histogram $N(\Delta\Theta_p)$ was used for the normalization.

The results of both the methods agree within experimental errors.

In the $\bar{p}p$ scattering the inelastic contribution is not important because of favourable momentum separation in the PT magnetic field.

IV. CROSS-SECTION CALCULATIONS

The differential elastic cross-section is given by

$$\frac{d\sigma}{dt} = C \frac{N_+(t) + N_-(t)}{\Delta t \cdot \epsilon(t)}, \qquad (1)$$

where $N_+(t)$, $N_-(t)$ are the numbers of elastic events in the momentum transfer intervals Δt with different signs of target polarization,

C is the normalization factor, $\epsilon(t)$ is the detection efficiency of the apparatus. The Monte Carlo method was used to calculate $\epsilon(t)$. In the calculation the following information was taken into account:

1) beam parameters ($\Delta p/p$, the horizontal and vertical divergences, shape and dimensions);

2) ionization losses, multiple scattering and absorption of the recoil protons in the target and surrounding materials;

3) cell dimensions in the incident beam, scattered particle and recoil proton hodoscopes H_1–H_9. The efficiency of scintillation counters was supposed to be independent of the momentum transfer t.

The programme includes a random choice of beam parameters, the scattering angle and the interaction point in the target and also a procedure showing the operation of coincidence selection matrices.

To simulate the real experimental situation this part of the programme gives a set of hodoscope $H_1 - H_9$ counter numbers at the output. Then the same reconstruction procedure is performed. According to the kinematic parameters of the events a t-distribution is constructed. Such a distribution per Δt unit describes the detection efficiency as a function of t. The detection efficiency for $\pi^- p$ scattering is shown in Fig. 3a. The oscillation about an average value is connected with the way the programme reconstructs the particle trajectories. It ascribes to the events a t-value corresponding to the centre of the involved cell of the hodoscope $H_{5,6}$. Consequently, the oscillation period is

$$\Delta t \simeq 2 \cdot P_{lab}^2 \cdot \frac{h}{L^2} d \quad (GeV/c)^2 , \qquad (2)$$

where d is cell vertical dimension, L is the distance from the target to the hodoscope $H_{5,6}$, h is the distance from the beam axis to the hodoscope cell, P_{lab} is the incident particle momentum.

The t-distribution of the experimental events has the same structure (Fig. 3b).

V. ABSOLUTE NORMALIZATION OF THE DIFFERENTIAL CROSS-SECTIONS

The optical theorem was used to normalize the differential cross section

$$\frac{d\sigma}{dt}\Big|_{t=0} = \frac{(\sigma^{tot})^2}{16\pi} . \qquad (3)$$

The total cross-section values were taken from ref.[4]. $\frac{d\sigma}{dt}$ was extrapolated to $t=0$ as $\frac{d\sigma}{dt} = A e^{bt+ct^2}$ by the least squares method considering $|t| \leq 0.5$ $(GeV/c)^2$ only. A more complex parametrization had to be used for a large $|t|$ region and the normalization was not changed within experimental errors.

VI. SYSTEMATIC ERRORS

The main source of systematic errors is the accuracy of the geometric parameters of the apparatus. The displacement of the beam hodoscopes H_1, H_3 is most important. If there is a vertical displacement Δz of H_3, it results in an error

$$\Delta t = 2 \cdot P_{lab}^2 \cdot \frac{h}{L^2} \Delta h , \qquad (4)$$

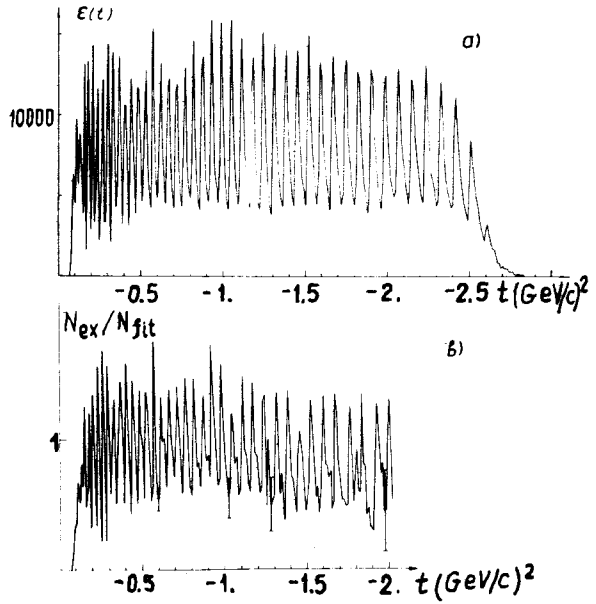

Fig. 3. a) Detection efficiency, $\epsilon(t)$, calculated by the Monte Carlo method. b) Experimental distribution $N_{exp}/N_{fit} = \epsilon(t)_{exp}$, where N_{exp} is the number of events in the t interval from the experiment, $N_{fit} = a \times \exp(Bt + Ct^2 + Dt^3)$ is a fit value of N_{exp}. The experimental statistical errors are shown at some points, as an example.

where $\Delta h = \frac{L}{L_1} \Delta z$ is a displacement of the beam axis in the hodoscope $H_{5,6}$ plane, L_1 is the distance from the beam hodoscope to the target.

Consequently the error in the calculated efficiency is

$$\Delta \epsilon(t) = \left| \frac{d\epsilon(t)}{dt} \right| \Delta t . \qquad (5)$$

If $\Delta z \simeq 2$ mm, the relative error amounts to smaller than 1% with $|t| > 0.15$ (GeV/c)^2. It increases rapidly with decreasing $|t|$.

Another source of systematic errors may be the inefficiency of the Cherenkov counter system. It gives a systematic error in the slope parameter b of $\bar{p}p$ and Kp differential cross-section ~ 1%.

VII. RESULTS

The differential cross-sections $\frac{d\sigma}{dt}$ versus $-t$ are shown in Figs. 4-9.

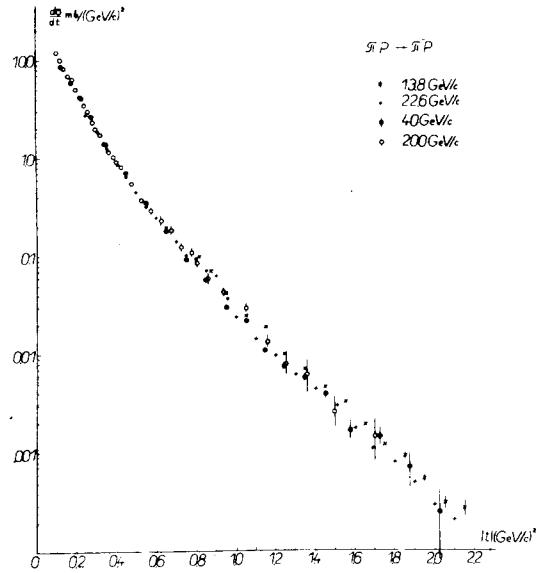

Fig. 4. Differential elastic cross-section for $\pi^- p$ *, + - ref.[5], o - ref.[6], • - this experiment.

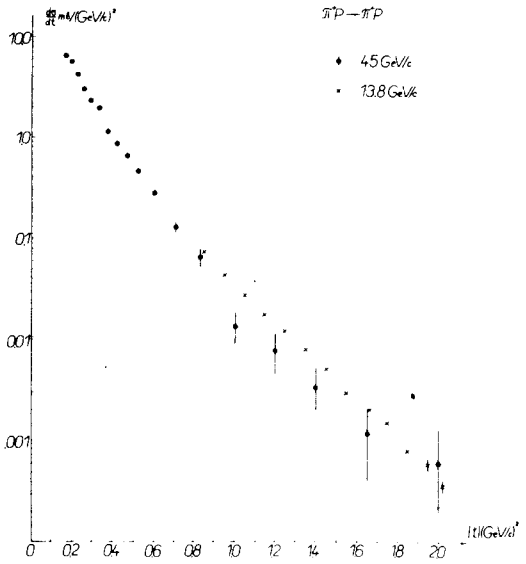

Fig. 5. Differential cross-section for π^+p * - ref./7/, ● - this experiment.

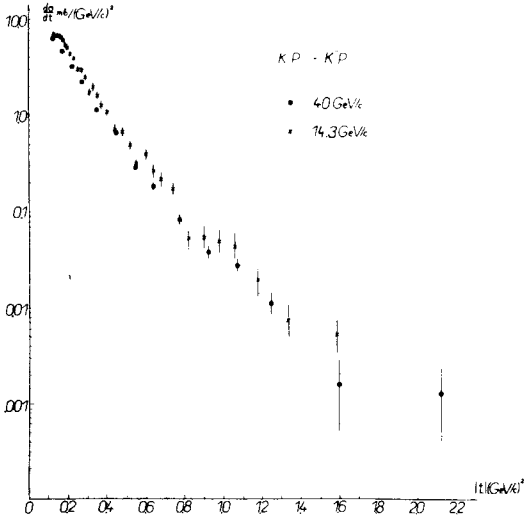

Fig. 6. Differential elastic cross-section for K^-p * - ref./8/, ● - this experiment.

Fig. 7. Differential elastic cross-section for K^+p * - ref./7/, o - ref./6/, ● - this experiment.

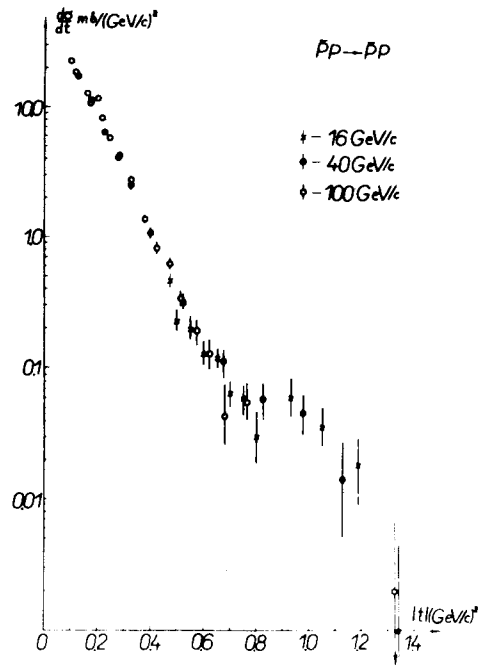

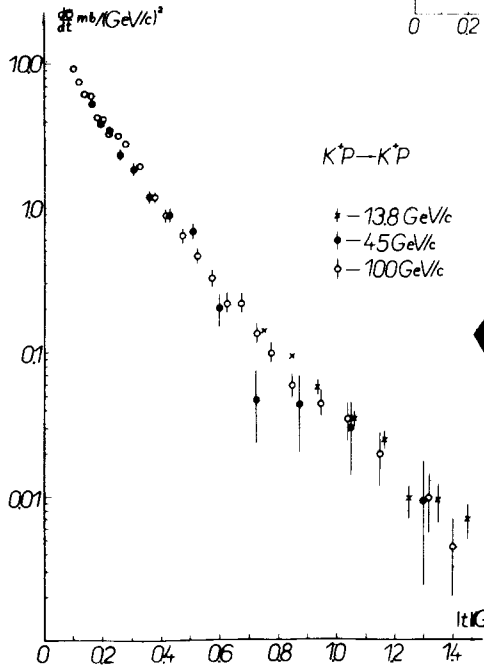

Fig. 8. Differential elastic cross-section for $\bar{p}p$ * - ref./9/, o - ref./6/, ● - this experiment.

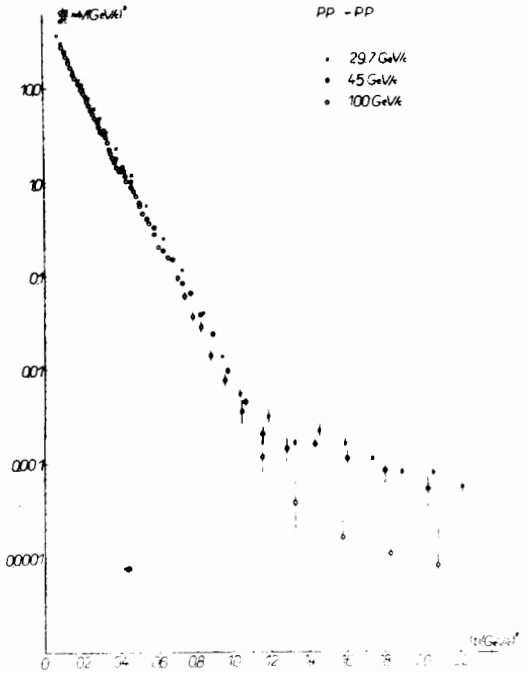

Fig. 9. Differential elastic cross-section for pp × - ref. /10/, o - ref. /11/, • - this experiment.

The differential cross-sections for $\pi^{\pm}p$, $K^{\pm}p$, $\bar{p}p$ were fitted with the exponential forms

$$\frac{d\sigma}{dt} = A \cdot \exp(bt + ct^2) \qquad (6)$$

$$\frac{d\sigma}{dt} = A \cdot \exp(bt + ct^2 + dt^3) \qquad (7)$$

$\frac{d\sigma}{dt}$ for pp was fitted by the following function:

$$\frac{d\sigma}{dt} = A \cdot \exp(bt + ct^2 + dt) + A' \exp(b't). \qquad (8)$$

The results are listed in the Table. It

Table

P_{lab} GeV/c		A mb/(GeV/c)^2	b (GeV/c)$^{-2}$	c (GeV/c)$^{-4}$	d (GeV/c)$^{-6}$	A' mb/(GeV/c)^2	b' (GeV/c)$^{-2}$	χ^2/Num. of points	σ_{tot} mb/(GeV/c)^2	B(0.2) (GeV/c)$^{-2}$	M-range (GeV/c)^2
π^-p	40	0.99±0.02	9.54±0.13	2.89±0.22	0.43±0.10			47.7/20	29.84±0.69	8.44±0.16	0.175÷2.2
		0.90±0.01	8.91±0.05	1.86±0.04				76.2/20	27.10±0.35		
π^+p	45	1.00±0.08	8.86±0.59	1.9 ±1.1	0.15±0.56			25.2/18	27.3 ±2.2		0.165÷2.0
		0.93±0.05	8.75±0.25	1.66±0.27				26.4/18	26.9 ±1.2	8.12±0.27	
K^-p	40	1.04±0.07	9.08±0.40	2.93±0.65	0.42±0.26			22.2/13	22.0 ±1.4		0.175÷2.125
		0.96±0.04	8.49±0.16	1.91±0.13				24.6/13	20.17±0.73	7.96±0.16	
K^+p	45	1.02±0.26	6.5 ±1.9	-1.7 ±4.0	-1.8 ±2.3			18.7/13	16.9 ±4.3		0.165÷1.30
		1.15±0.16	7.71±0.77	1.15±0.91				19.0/13	19.6 ±2.7	6.96±0.85	
$\bar{p}p$	40	1.14±0.22	13.2 ±1.5	5.0 ±3.3	0.3 ±1.9			11.0/11	115 ±21		0.175÷1.325
		1.11±0.10	13.00±0.52	4.54±0.61				11.1/11	113 ±10	11.24±0.57	
pp	45	1.12±0.05	11.38±0.37	4.18±0.90	2.23±0.67	$(2.7\pm2.2)\cdot 10^{-5}$	0.49±0.39	54.0/27	85.1±3.8	9.98±0.52	0.165÷2.05

follows from the Table that the channels with better statistics and the large t-interval (π^-p) need a more complicated parametrization. As for the π^+p and Kp -scattering data the parametrization (7) is satisfactory.

It may also be seen that the parameters b, c are in agreement with the results of other experiments [12,13,14] at close energies.

The Table also includes the logarithmic slope parameters defined as

$$B(|t|) = \frac{d}{dt}\left(\ln \frac{d\sigma}{dt}\right) = b - 2c|t| + 3d|t|^2 \qquad (9)$$

evaluated at $|t| = 0.2$ (GeV/c)^2.

Now consider in some detail [15] the t- and s - dependence of the differential cross sections resulting from our data.

The t-dependence of the elastic $\pi^\pm$p and $K^\pm$p differential cross sections is plotted in Figs. 10,11 in a double logarithmic scale. It shows in a wider interval of t ($0.5 \leq |t| \leq 2$)GeV/c)^2), the power law of the t - dependence, which has been noted at higher energies earlier [16].

The s -dependence of $d\sigma/dt$ at some fixed values of t is shown in Figs. 12-14. The solid straight lines show the energy slope at our energy which has been calculated [15] in accordance with the geometrical scaling hypothesis, GS, [16,19]. One can see that in the experimental error limits the p and Kp data are in agreement with GS predictions up to $|t| = 2$ (GeV/c)^2.

The universal GS-dependence of $\frac{d\sigma}{dt} / \frac{d\sigma}{dt}\Big|_{t=0}$ on $(t \cdot \sigma_{tot})$ has been found for $\pi^\pm$p and $K^\pm$p scattering at $P_{lab} = 100$-200 GeV/c earlier. Our data at 40 GeV/c confirm the universality also (Fig. 15).

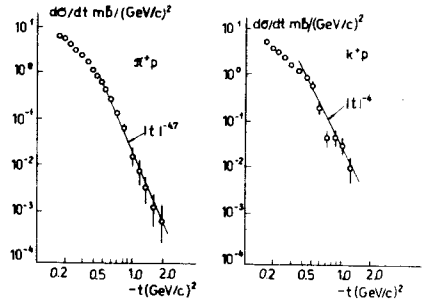

Fig. 10. Approximate $(d\sigma/dt) \sim t^{-\lambda}$ shape for π^-p, K^-p differential cross-section in the range of $|t| \approx 0.5$ to 2.0 (GeV/c)^2.

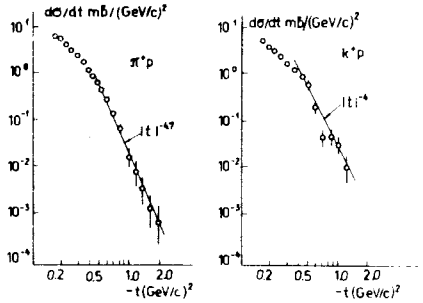

Fig. 11. The same as in Fig. 10 for π^+p, K^+p.

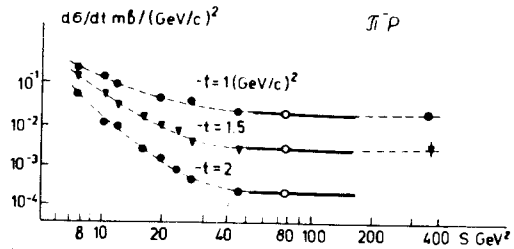

Fig. 12. The s-dependence of $d\sigma/dt$ for π^-p scattering for a fixed value of t. ●, ▼ - ref. [5,6] o - this experiment, ——is the predictions of GS, ---- are to guide the eye.

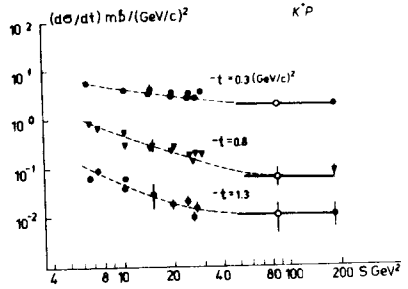

Fig. 13. The same as in Fig. 12 for K^+p scattering ●, ▼ - ref./7,17/ o - this experiment.

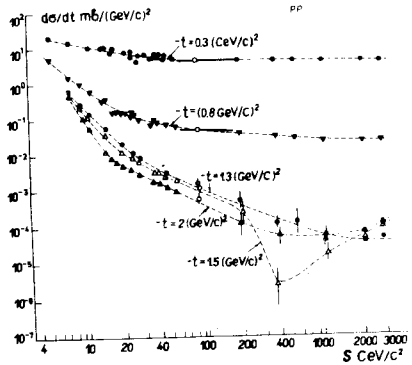

Fig. 14. The same as in Fig. 12 for pp - scattering ● ▼ ▲ Δ - ref./10,11,18/, o - this experiment.

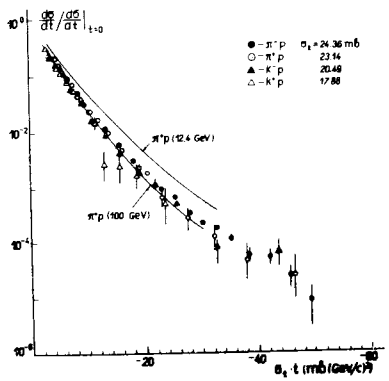

Fig. 15. Test of geometrical scaling. Experimental points are the results of this experiment. Solid curves reproduce the behaviour of experimental data at 12.4 GeV/c and 100 GeV/c /6/ for π^+p -scattering.

GS is heavily violated in pp scattering for $|t| \gtrsim 1$ (GeV/c)^2 (Fig. 14). The reason of the violation is a Reggeon contribution which gives the following correction to the energy slope of $d\sigma/dt$, ref./15/

$$\left(\frac{d\left(\ln \frac{d\sigma}{dt}\right)}{d(\ln s)}\right)_{Regge} \sim [\alpha_{eff}(t)-1]\delta(s,t). \qquad (10)$$

Here $\alpha_{eff}(t)$ is an effective Regge trajectory describing the energy dependence of the Reggeon contribution, $\delta(s,t)$ is defined as follows:

$$\delta(s,t) = \frac{\frac{d\sigma}{dt}(\bar{x}p) - \frac{d\sigma}{dt}(xp)}{\frac{d\sigma}{dt}(\bar{x}p) + \frac{d\sigma}{dt}(xp)}, \qquad (11)$$

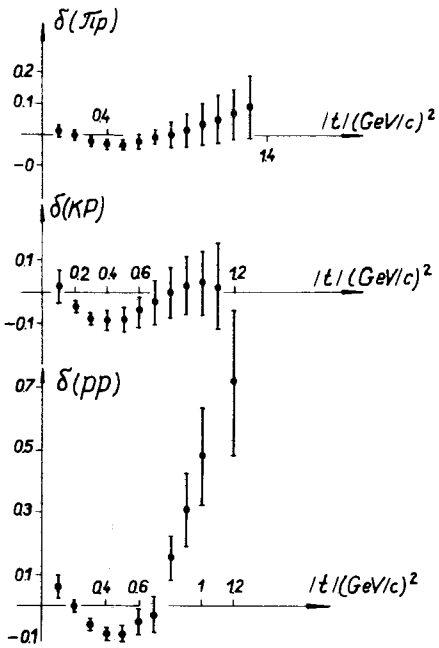

Fig. 16. The values $\delta(t)$ defined by eq. (11) in the text for $\pi^{\pm}p$, $K^{\pm}p$, $p^{\pm}p$ scattering.

where $\frac{d\sigma}{dt}(xp)$ and $\frac{d\sigma}{dt}(\bar{x}p)$ are the particle- and antiparticle-proton scattering cross-sections, respectively. The values of $\delta(s,t)$ for different reactions calculated from our data are shown in Fig. 16. For $\pi^{\pm}p$ and $K^{\pm}p$ scattering $\delta(s,t)$ is about 5-10%. Consequently, the deviation from the GS prediction is within experimental errors[15]. It can be seen that $\delta^{pp}(s,t)$ increases rapidly for $|t| \gtrsim 1$ (GeV/c)^2. So, the correction (10) becomes large and GS is violated, as it has been mentioned above.

REFERENCES

1. A.Gaidot et al. Phys.Lett., 57B, 389 (1975).
   A.Gaidot et al. Phys.Lett., 61B, 103 (1976).
2. J.Pierratd et al. Phys.Lett., 57B, 393 (1975).
   J.Pierrard et al. Phys.Lett., 61B, 107 (1976).
3. J.C.Raoul et al. Nucl.Instr. and Meth., 125, 585 (1975).
4. S.P.Denisov et al. Phys. Lett., 36B, 528 (1971).
   Y.P.Gorin et al. Phys.Lett., 36B, 415 (1971).
5. P.Cornillon et al. Phys.Rev.Lett., 30, 403 (1973).
6. C.W.Akerlof et al. Phys.Rev.Lett., 35, 1406 (1975).
7. R.Rubinstein et al. Phys.Rev.Lett., 30, 1010 (1973).

8. R.J.Miller et al. Phys.Lett., 34B, 230 (1971).
9. D.Birnbaum et al. Phys.Rev.Lett., 23, 663 (1969).
10. R.M.Edelstein et al. Phys.Rev., D5, 1073 (1972).
11. C.W.Akerlof et al. Phys.Lett., 59B, 197 (1975).
12. Yu.M.Antipov et al. Nucl.Phys., B57, 333 (1973).
13. Yu.M.Antipov et al. Preprint IHEP 74-99, 1974.
14. D.S.Ayres et al. Phys.Rev.Lett., 35, 1195 (1975).
15. I.K.Potashnikova. JINR, P2-10073, Dubna, 1976.
16. V.Barger, J.Luthe, R.J.Phillips. Nucl. Phys., B88, 237 (1975).
17. W. De Baere et al. Nuovo Cim., 45, 885 (1966).
    C.Y.Chien et al. Phys.Lett., 28B, 615 (1969).
    P.L.Jain et al. Nucl.Phys., B19, 568 (1970).
    C.W.Akerlof et al. Phys.Rev.Lett., 26, 1278 (1971).
    V.Chabaudet et al. Phys.Lett., 38B, 445 (1972).
    R.K.Carnegie et al. Phys.Lett., 59B, 308 (1975).
18. A.Böhm et al. Phys.Lett., 49B, 491 (1974).
19. V.Barger, Rapporteur talk, Proc. London Conf., 1974.
20. D.Harting et al. Nuovo Cim., 38, 60 (1965).

Received by Publishing Department
on August 25, 1976.